DOI 10.1590/s1982-21702024000100012

ORIGINAL ARTICLE

A new approach to satellite-derived bathymetry: the use of NDWI and ANN with bathymetry sections for reservoir mapping

Laura Coelho de Andrade[1] - ORCID: 0000-0003-3693-2208

Letícia Perpétuo Pinheiro[1] - ORCID: 0000-0002-4572-6847

Italo Oliveira Ferreira[1] - ORCID: 0000-0002-4243-8225

Nilcilene das Graças Medeiros[1] - ORCID: 0000-0003-0839-3729

Arthur Amaral e Silva[1] - ORCID: 0000-0001-5548-459X

[1] Universidade Federal de Viçosa, Departamento de Engenharia Civil, Viçosa – Minas Gerais, Brazil.
E-mail: laura.andrade@ufv.br; leticiaperpetuopinheiro@gmail.com; italo.ferreira@ufv.br; nilcilene.medeiros@ufv.br; arthuramaral.e.a@gmail.com

Received in 26th May 2023.
Accepted in 17th May 2024.

Abstract:

Mapping the submerged bottom is a hampered task when traditional vessels are inserted in shallow places that pose a danger to navigation. In this sense, current research has sought optical remote sensing to obtain bathymetry estimates in larger locations in less time. However, most studies employ a large sample of bathymetric points to estimate depth with orbital images. The need for a large amount of random bathymetric points can make these procedures less viable and unattractive. Thus, the present work proposes a methodology to estimate bathymetric depths from orbital images using sections of bathymetric points previously spaced in the study area, avoiding the need for a high amount of points collected through traditional bathymetric surveys. This work also compares this methodology using the NDWI index and the ANNs. Furthermore, the study showed that the points contained in the sections are quite efficient for extracting bathymetry with orbital images, especially through the implementation of neural networks, achieving a volume estimation accuracy within 4% of the actual volume of the reservoir in question.

Keywords: Remote Sensing; Bathymetric Sections; Artificial Intelligence; Inland Waterbodies.

How to cite this article: ANDRADE LC, PINHEIRO LP, FERREIRA IO, MEDEIROS NG, SILVA AA. A new approach to satellite-derived bathymetry: the use of NDWI and ANN with bathymetry sections for reservoir mapping. *Bulletin of Geodetic Sciences*. 30: e2024012, 2024.

1. Introduction

Water is essential for the survival of all living organisms on earth. It is an indispensable resource for agriculture, industry, and human consumption, playing a crucial role in regulating the Earth's climate, acting as a thermal buffer that helps moderate temperature extremes (Hallsworth,2022). Furthermore, water serves as a habitat for aquatic organisms and contributes to the overall health of ecosystems (Jackson et al. 2001). In addition, it is a vital component in producing energy, such as hydroelectric power (Silva & Perreira,2019). The importance of water cannot be overstated, as its scarcity or contamination can devastate human health and the environment. Therefore, it is essential to conserve and protect this resource for current and future generations (Qaddumi, 2008). Additionally, water resources are indispensable for supporting basic sanitation infrastructure, including sewage systems and wastewater treatment plants, which mitigate water contamination and the spread of waterborne diseases, further enhancing public health outcomes. Furthermore, water is instrumental in agricultural practices, serving as a vital component for irrigation, livestock watering, and food production. Its availability directly impacts agricultural productivity, food security, and local economies. Moreover, water is integral to industrial processes across various sectors (Hamdy,2007; Piao et al. 2010; Dhawan,2017).

According to Matos (2012), reservoirs are important in capturing water and, consequently, managing water resources. Therefore, the study of these systems' volume can provide results and information regarding the silting of the site and consequently make it possible to monitor anomalies and future problems with the supply.

Bathymetric surveys are commonly used to determine the volume of reservoirs. To this end, equipment such as the echo sounder is used, whose principle is sound propagation in water. This tool can be SBES (Single Beam Echo Sounder) or MBES (Multi Beam Echo Sounder). Together with the bathymetric equipment, instruments are used for planimetric positioning, such as the GNSS (Global Navigation Satellite System), obtaining georeferenced depths of the site, allowing the determination of the reservoir's volume (IHO,2005; Jong et al.,2010; Ferreira et al.,2016a).

In a singlebeam bathymetric survey, the area to be studied should be divided into a mesh of equidistant lines previously established. These lines can be parallel, circular, radial, or zigzag, called regular-sounding lines (Ferreira, 2015). When using the parallel lines model, these must be drawn according to the isobathymetric lines of the study area. According to Martini (2007), for singlebeam systems, the regular-sounding lines must be perpendicular to the river thalweg or, in the case of ponds, to the bank. It should be noted that the spacing between the lines may vary if the submerged relief has many irregularities.

However, traditional surveys have a high cost and demand a long time to execute in the field. The emergence of equipment such as the USV (Unmanned Surface Vehicle), ASC (Autonomous Surface Craft), and ASV (Autonomous Surface Vehicle) added to the advances in the technological scope of hydrographic surveys; there were improvements in data collection in hard-to-reach places, as well as in places that posed risks to operators or that had low depth. In addition to minimizing the cost and data collection time in the field (Manley,2008; Giordano et al.,2015; Ferreira et al.,2016a). The use of remote sensing in bathymetry has also been shown to be a viable technique for obtaining depths with the technology's progress. It has risen due to its practicalities, especially in shallow water locations. Bathymetry extraction using orbital imagery is based on the principle that the intensity of radiant energy reflected by a water column and received by the sensor is a function of water depth, that is, the portion of solar radiation that has penetrated the water column. With this method, data can be rapidly collected over large areas cheaply (Legleiter et al., 2009; Candela, 2013).

Several studies propose this methodology combined with other parameters to obtain bathymetry in water bodies. Zani et al. (2008) carried out a study in the Paraguay River with the ASTER sensor, where they used the pixel value of the band with the best correlation with the data found in the field to estimate the depth. Besides these, Foerstnow & Menezes (2011) and Lima et al. (2012) used orbital images of the Landsat system, together with the NDWI index (Normalized Difference Water Index, to obtain bathymetry in shallow waters through the combination of bands (green light and near-infrared). Ferreira et al. (2016b) used the RapidEye system with NDWI to estimate the bathymetry of a reservoir in Viçosa – MG, Brazil and could reach an uncertainty of 1 meter. Poursandis et al. (2019) used PlanetScope images on the island of Crete to estimate the bathymetry. They found a low vertical uncertainty for a depth of 10 m, which fits the requirements proposed by the International Hydrographic Organization. Ma et al. (2020) used Sentinel 2 images and ICESat-2 lidar points associated with the band ratio model and linear band model to estimate bathymetry, finding an RMSE (Root Mean Square Error) of approximately 1 m. Finally, Santos et al. (2022) used Sentinel 1 images to determine the bathymetry of the Portuguese coast and found an uncertainty of 2 m for a depth of 10 m.

In addition, Artificial Neural Networks (ANN) have been used as a methodology capable of improving the estimates made with satellite images. This method simulates part of the human brain with mathematical equations and weighted numerical values (Huang et al., 2007). For example, Ribeiro et al. (2008) used a multilayer supervised ANN to obtain, through an image of the IKONOS II system, with the green and red bands, a depth model for the studied region. According to the authors, the results show a difference of only 0.25-0.50 meters between the ANN results and the reference.

El-Mewafi et al. (2018) employed a multi-layer feed-forward neural network in conjunction with other techniques such as binary classification and Inverse Probability Weighted Interpolation on Landsat 8 images, achieving an average error of 0.46 m for areas at a depth of 4.5 meters. Kaloop et al. (2021) created a hybrid ANN method called OPELM (Optimally Pruned Extreme Learning Machine) that is capable to derive bathymetry from Sentinel 2A images with a superior accuracy from traditional ANN and the traditional Stumpf model by 18.76% and 32.46%. Guo et al. (2022) utilized Sentinel 2A imagery along with the Backpropagation method for neural networks and ICESAT-2 data for training, achieving an RMSE between 0.97 and 1.43, surpassing the multi-band ratio method. Andrade et al. (2022) also used ANN to estimate the bathymetry of reservoirs using RPA's (Remotely Pilot Aircrafts) and obtained estimates with errors smaller than one meter.

However, it is known that this methodology used to extract the bathymetry by spectral response has as input numerous random points throughout the study area, containing the reference depth (collected by acoustic methods *in loco*). The fact that the method requires a large number of points causes some difficulty in execution since the data collection in a bathymetric survey using an echo sounder is time-consuming and requires some experience from the operator, especially in places with currents and for long water courses, such as rivers.

Thus, using a few bathymetric sections with pre-defined spacing appears viable to improve the bathymetry extraction methodology by the spectral response. In this way, the input sample contains few points with the reference depth, considerably reducing the time spent in a bathymetric survey. In this context, the main objective of this study is to evaluate the bathymetry extraction through a high-resolution orbital image using sections of bathymetric points instead of a mesh of random points.

2. Materials and Methods

2.1 Study Area

Our research focuses on the Casquinha Dam reservoir situated in Canaã, Minas Gerais (Figure 1), where we conducted field surveys to gather depth data. In addition to field measurements, orbital imagery of this area was also utilized. It is noteworthy that since its inception in 1960, ownership of the reservoir has been vested in the Federal University of Viçosa (UFV).

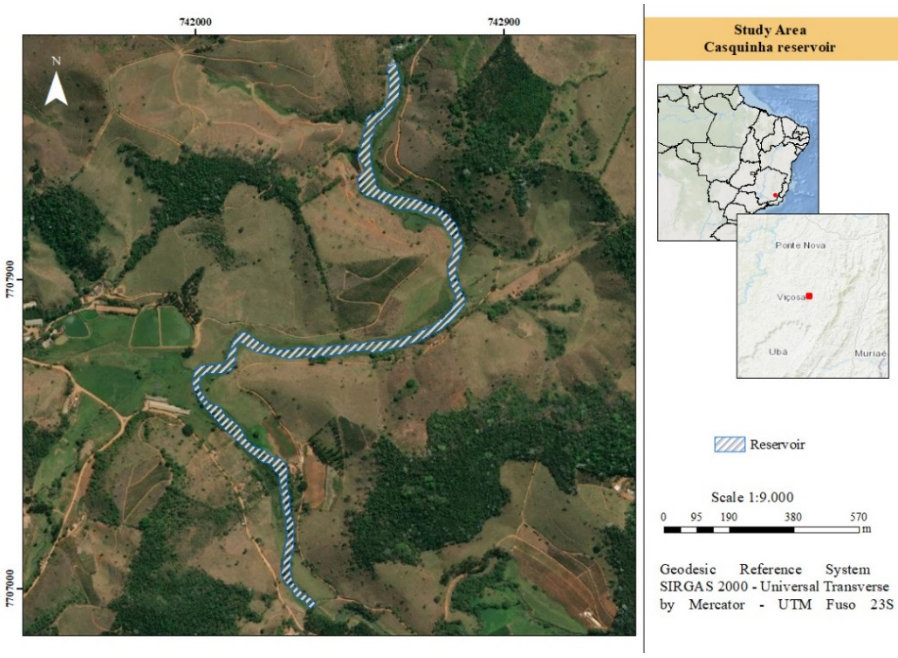

Figure 1: Location map of the Casquinha Dam Reservoir.

The author used an area of approximately 6.5 ha in this research. The restitution of this data was performed in ArcGIS software through the RPA image photo interpretation site. This area was selected to assist in future projects foreseen by the university, which aim to use the Casquinha Dam reservoir as its independent electrical power source. It is necessary to mention that the reservoir has a minimum width of 3 meters and a maximum of approximately 25 meters and a maximum depth of approximately 6 meters and a minimum of almost 0.3 meters.

A flowchart was prepared to facilitate the understanding of the proposed methodology (Figure 2), and also a table containing the acronyms of some words used in the text (Table 1).

Table 1: Models' calculated volumes (N150, N250, N500, Ntrad, and reference bathymetry).

	Meaning
N150	NDWI with sections spaced by 150 m
N250	NDWI with sections spaced by 250 m
N500	NDWI with sections spaced by 500 m
Ntrad	NDWI with random points
A150	ANN with sections spaced by 150 m
A250	ANN with sections spaced by 250 m
A500	ANN with sections spaced by 500 m
Atrad	ANN with random points
XYZ_{bat}	Reference bathymetry

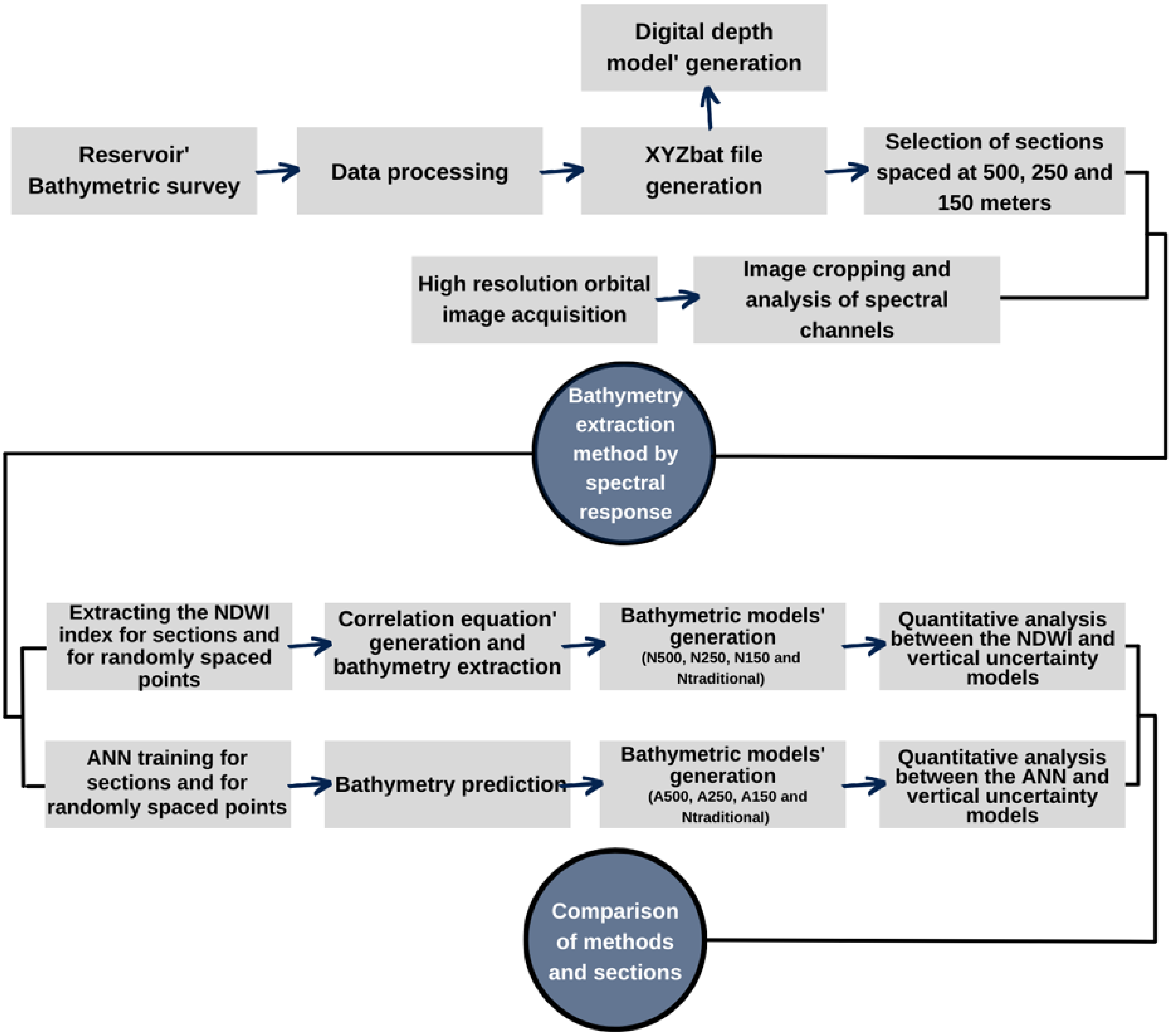

Figure 2: Methodological flowchart.

For this study development, the PlanetScope Ortho Scene image was used from the Dove sensor. It has post-processing already applied (Planet, 2016). The product is radiometrically and geometrically corrected. It is available to the user with an approximate geometric resolution of 3m. It should be noted that the image acquired is from April 2020, with less than 10% cloud cover, and there was a need to cut it to contemplate the reservoir area. The cut was intended to maximize the computational efficiency necessary for product generation.

In addition to the image, a reservoir bathymetric survey was carried out (April 2020), following the standards proposed by the ANA (2013), which states that the maximum spacing of transverse and longitudinal lines for small hydroelectric power plants should be based on the area and extent of the reservoir at its normal operational level.

The authors used a singlebeam echo sounder equipped with a 200 kHz transducer to collect the depths. It used a GNSS receiver with L-band correction, with nominal accuracy better than 10cm, to acquire geodetic coordinates. After collection, the Hypack software performed data processing (Hypack, 2018), which resulted in a data file containing the X, Y, and Z coordinates of the points (XYZ_{bat}), also called reference bathymetry.

Considering that the mesh of points resulting from the processing does not represent the relief continuously, a digital model of the reservoir's depth was generated for XYZ_{bat} using the universal kriging interpolator. Santos

(2011) states this technique should be used when a trend is detected in the data. Thus, this technique removes the trend through a low-degree polynomial adjustment. Furthermore, as evidenced by Ferreira, Rodrigues, and Santos (2013), Andrade et al. (2018), and Santos et al. (2018), this interpolator presents better predictions for the same scope of the study. Therefore, this model was used as a reference throughout this study for statistical analyses. Then, sections of bathymetric points spaced at 150, 250, and 500 meters along the reservoir were manually selected.

2.2 Bathymetry extraction method by NDWI

With the bathymetric sections previously defined and spaced at 150, 250, and 500 meters, a sample of points was used to extract the NDWI index from the image, thus creating the correlation equations through the regression model that best fitted the data (values obtained with the NDWI index and the depths, in the Excel software), such as Krug and Noernberg (2009), Ferreira et al. (2016b) and Andrade et al. (2021).

It is worth noting that the innermost points of the water body were filtered to minimize noise in the prediction, excluding those located in edge pixels. The NDWI was calculated using the Equation 1 (Mcfeeters, 1996).

$$\mathrm{NDWI} = \frac{\rho Green - \rho Nir}{\rho Green + \rho Nir} \tag{1}$$

The extraction of the index was carried out using the sample of bathymetric points obtained randomly through the tool for random point selection in ArcGIS software, so it was possible to compare the proposed methodology and the extraction of bathymetry by the spectral response in the traditional way (choosing points randomly along the reservoir)

Therefore, these equations were used to estimate bathymetry through the radiance values of the green and near-infrared bands. In sequence, four digital depth models were generated with different section spacings (N150, N250, and N500) and also for the traditional method (placed as Ntrad), using the universal kriging interpolator (Andrade et al., 2022). For this work, the traditional method mentioned refers to the one in which random points distributed in the study area are used to determine the bathymetry by the spectral response. The reference method, or reference bathymetry, is collected using an echo sounder.

Statistical analysis was carried out to verify the models' vertical uncertainty by selecting some random points of the reference bathymetry (XYZ_{bat}), which was not previously used, subtracted from the bathymetry estimated by each Digital Depth Model (DDM), using a methodology developed and proposed by Ferreira et al. (2018), called MAIB (Methodology for Assessing the Uncertainty of Bathymetric Data) in an R environment (R core team, 2020). It is noteworthy that the volume calculation of each DDM built was also carried out to compare the generated models with the one obtained through the bathymetric survey using an echo sounder.

2.3 Bathymetry extraction method by ANN

For the prediction of bathymetry by orbital image using ANNs, the three sections (150,250 and 500) were used for network training by the "neuralnet" package (R software) and the random point sample. It is noteworthy that this package uses the backpropagation tool in learning. Thus, through the spaced sections, 80% of the points are for training and 20% for network evaluation. The network architecture had six input layers (the values of the Blue, Green, Red, and Near Infrared bands and the values of the coordinates East and North of each point), three hidden layers, and only one output layer; in this case, the estimated depth.

In sequence, the creation of DDMs (A150, A250, A500, and Atraditional) was carried out for the estimated depths with the respective section spacing and the random points of the bathymetry extracted by the spectral response. The traditional method mentioned refers to the one in which random points distributed in the study area are used to determine the bathymetry by the spectral response.

The models were also generated using universal kriging (Andrade et al., 2022), and their volumes were calculated for a comparative analysis of the ANN DDMs. To verify the model uncertainty, the same procedure performed for the NDWI index was used for ANN, that is, through the MAIB algorithm.

Finally, it was also evaluated which method presented the lowest vertical uncertainty according to the methodology discussed, NDWI and ANN, verifying which of these methods came closest to the real reservoir volume, that is, calculated based on the bathymetric model generated with XYZ_{bat}, while finding the most suitable section spacing for the study area.

3. Results and Discussion

From the cropped image and the corresponding spectral bands related in the ArcGIS software, the processed data of the bathymetric survey called XYZbat were superimposed on the image to determine the sections of approximately 150, 250, and 500 meters, as shown in Figure 3.

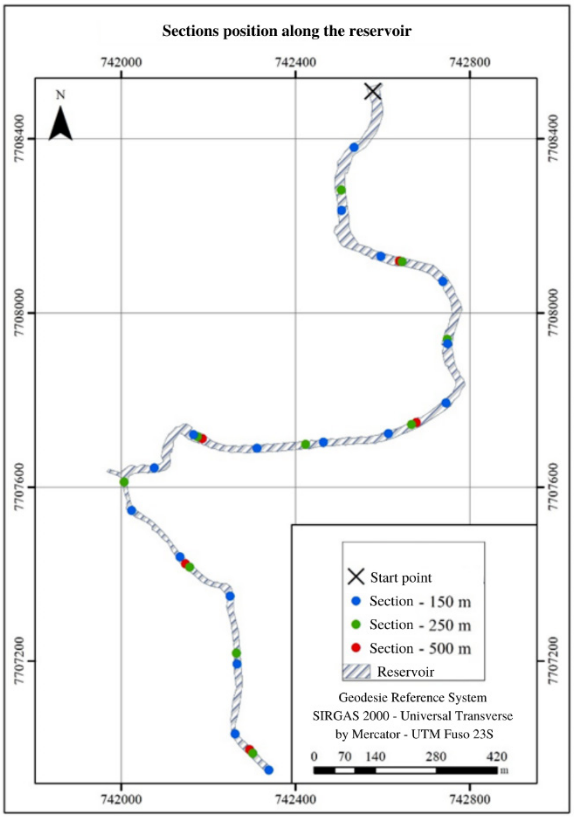

Figure 3: Sections along the reservoir.

Following the proposed methodology, geostatistical modeling was carried out based on universal kriging for the points obtained in the XYZ_{bat} reference bathymetric survey, obtaining the reference MDP. It is noteworthy that the adequate modeling of the semivariogram has a direct influence on the resulting interpolation; therefore, this step was carried out closely, following the recommendations of Vieira (2000).

3.1 Bathymetry extraction method by NDWI

Using the NDWI index to extract the bathymetry, it was possible to generate the regression models that best fit each data set. Figure 4 summarizes the equations and correlation coefficient (R^2) found for each spacing and the traditional method.

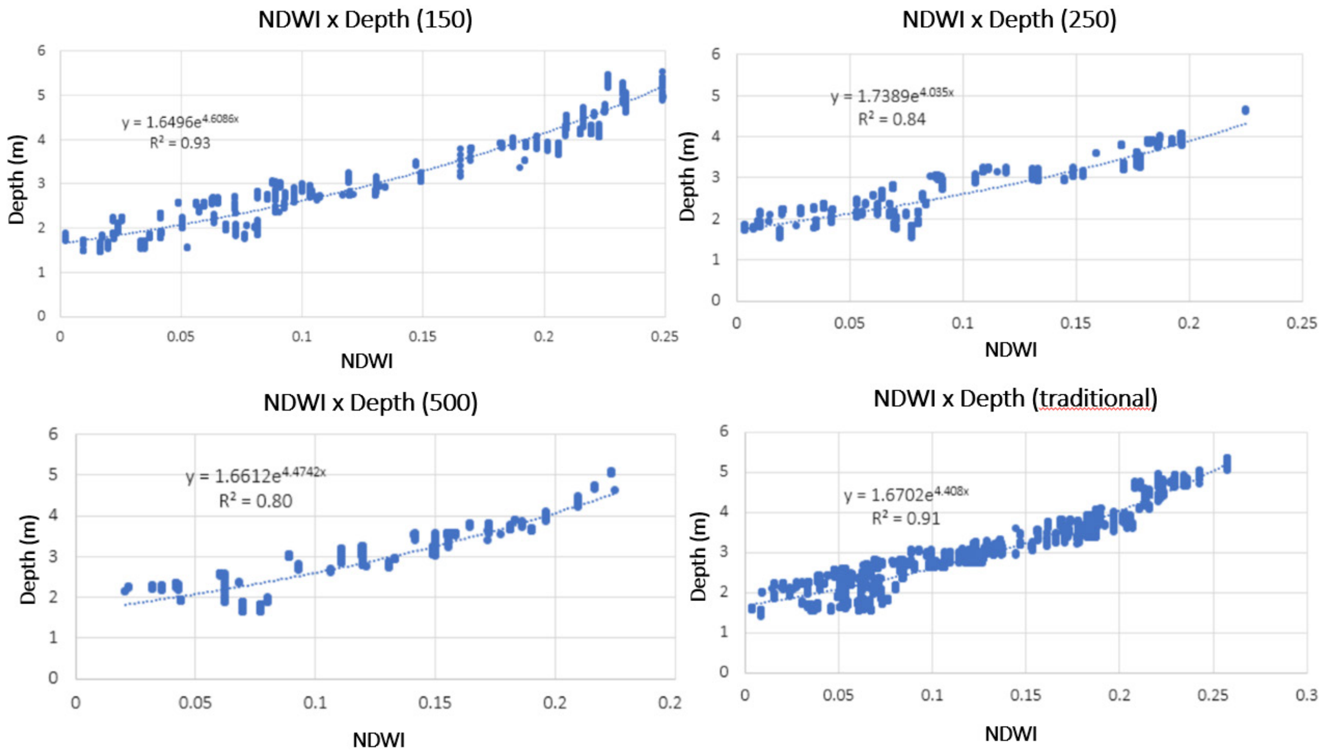

Figure 4: Correlation equations and R^2 values for each data set.

As can be seen in Figure 4, the exponential model was the best fit. This equation can characterize up to 93% of the spectral response variation. Authors such as Ferreira et al. (2016b) found a correlation coefficient of 89% for bathymetry estimation using NDWI in a reservoir with similar conditions. It is noteworthy that the polynomial, logarithmic, and linear models were tested for this study; however, they did not present sufficiently high R^2 values for the data studied.

It is important to mention that in the areas near the reservoir's shores, anomalous pixel values were observed, which harmed the results. Therefore, these points were excluded from the training data for all the sections under study to preserve the spectral response of the body of water.

Thus, it was possible to estimate the reservoir depth for all existing pixel values using equations 2, 3, 4, and 5, representing the N150, N250, N500, and Ntrad methods.

$$Z = 1.6496 * \exp(4.6086 * \mathrm{NDWI}) \tag{2}$$

$$Z = 1.7389 * \exp(4.035 * \mathrm{NDWI}) \tag{3}$$

$$Z = 1.6612 * \exp(4.4742 * \mathrm{NDWI}) \tag{4}$$

$$Z = 1.6702 * \exp(4.408 \ * \ \mathrm{NDWI}) \tag{5}$$

Where Z is the depth to be estimated, and NDWI is composed of the radiance values of the NIR (Near Infrared) band and the green band.

The universal kriging tool was used again for the sample of points to generate the bathymetric models (N150, N250, N500, and Ntrad), thus calculating the volume through these generated models. Table 2 summarizes the values obtained compared to the volume found for the bathymetry performed with an echo sounder (Reference Bathymetry).

Table 2: Models' calculated volumes (N150, N250, N500, Ntrad, and reference bathymetry).

	Volume (m³)	**Difference with the reference method (m³)**	**Difference with the reference method (%)**
N150	109,927.181	4,976.598	4%
N250	85,306.215	29,597.555	26%
N500	66,495.772	48,408.998	42%
Ntrad	102,077.450	12,826.32	11%
Reference Bathymetry	114,903.770	-	-

Through the existing volumes presented in Table 2, it is possible to affirm that the one that showed the smallest difference from that obtained by the reference bathymetry was the N150, with 4,977 m³ less. Ntrad also demonstrated accurate volume prediction, with a mere 11% difference from the reference bathymetry. This occurrence highlights the effectiveness of employing a greater number of closely spaced sections in the area to achieve precise volume calculations. In contrast, the sections spaced 500 meters did not yield accurate volume predictions, exhibiting a substantial 42% error.

For a more robust analysis of the bathymetry's vertical quality found with the respective sections and by the reference method, authors used the MAIB algorithm in a sample of random points of XYZ_{bat}, subtracted from the depth values for the respective generated models. It is noteworthy that Ferreira et al. (2021) also used this method for multibeam bathymetric data. Thus, it was possible to find the following exploratory analysis for the discrepancies (Table 3).

Table 3. Exploratory analysis of discrepancies for the method using NDWI.

	N150	**N250**	**N500**	**Ntrad**
Nº of observations	2107	1590	946	5522
Mean (m)	0.592	0.928	1.373	0.650
Minimum (m)	0.000	0.000	0.000	0.000
Maximum (m)	3.028	3.243	4.670	3.893
Variance (m²)	0.230	0.237	0.617	0.216
Kurtosis coefficient	1.636	0.012	0.189	0.647
Asymmetry coefficient	1.285	0.293	0.489	0.851

By analyzing the data (Table 3), it can be seen that the kurtosis coefficient is less than 3, characterizing a platykurtic and symmetrical distribution since the asymmetry coefficient indicates the deviation concerning a symmetrical distribution. According to the variance, it is also noted that the data have high variability (Warrick & Nielsen,1980), especially for N500.

Following the algorithm execution, it is necessary to examine the data's spatial autocorrelation and distribution to construct good confidence intervals. According to Santos (2015), the sample must be spatially independent for applying univariate normality tests, such as those of Shapiro-Wilk and Kolmogorov –Smirnov. So, evaluating the sample's spatial autocorrelation is necessary to understand the data normality.

Thus, the next step is the independence analysis through the experimental semivariogram, a geostatistical tool to verify this characteristic in the sample. In the methodology used, four semivariograms are usually constructed, with ranges equal to 100%, 75%, 50%, and 25% of the maximum distance. Through the analysis of these graphs, it is concluded that the discrepancies are spatially dependent, with a strong spatial dependence according to the classification proposed by Cambardella et al. (1994) ($\frac{N\text{ugget effect}}{Sill} < 0{,}25$).

After verifying the data dependence, the next step, following the methodology proposed in Ferreira (2018), is the Block Bootstrap application to estimate confidence levels. This step considered 5,000 replications. That is, the technique establishes 5,000 new data sets and inserts values corresponding to the range of the experimental semivariogram for the diagonal of the block. The histograms and QQ Plot graphs of the samples constructed for the estimators Φ (Uncertainty), Root Mean Square Error (RMSE), and Φ_{Robust} (Robust Uncertainty), the latter being also proposed by Ferreira (2018), are found in Supplementary Materials A, B, C and D for N150, N250, N500 and Ntrad respectively.

Calculating the sample bias, which, according to Ferreira (2018), is determined through the difference between the estimated uncertainty through the original sample and the median of the Bootstrap data, was possible to evaluate the Block Bootstrap estimates (Table 4).

Table 4: Vertical uncertainty at the 95% confidence level and Bootstrap bias.

	Estimator	Vertical uncertainty	$IC_{95\%}$	Sample bias
N150	RMSE (m)	0.772	(0.767 – 0.778)	-0.011
	Φ (m)	0.772	(0.767 – 0.778)	-0.011
	Φ_{Robust}	0.705	(0.698 – 0.711)	-0.010
N250	RMSE (m)	1.014	(1.010 - 1.018)	0.034
	Φ (m)	1.014	(1.010 - 1.018)	0.034
	Φ_{Robust}	1.052	(1.048 - 1.059)	0.017
N500	RMSE (m)	1.459	(1.454 - 1.467)	0.122
	Φ (m)	1.459	(1.454 - 1.467)	0.122
	Φ_{Robust}	1.359	(1.351 - 1.369)	0.201
Ntrad	RMSE (m)	0.803	(0.799 - 0.807)	0.003
	Φ (m)	0.803	(0.799 - 0.807)	0.003
	Φ_{Robust}	0.773	(0.765 - 0.777)	-0.031

The Bootstrap samples generated have low values for the bias of all estimators, especially for Φ_{Robust} concerning the Ntrad methods.

From Table 4, it is also evident that smaller uncertainty values were obtained with N150, approximately 0.770 m, while for the traditional method, this value was 0.803 m, with a difference of 30 cm. These values align with the observed volume values in Figure 3 for the R^2

Higher uncertainties are also observed for data generated from spaced sections of 250 and 500 meters, reaching an error of 1.459 m for N500. This phenomenon is consistent with the volume value found in Table 2.

It is worth noting that studies utilizing NDWI for bathymetry estimation in water bodies with a maximum depth of 4.5 m reported uncertainties ranging from 1.0 m to 3.5 m (Krug & Noernberg, 2007) and 0.7 m for reservoirs up to 3.0 m in depth (Andrade et al., 2021), similar to the results found in this study. Ferreira et al. (2016b) and Andrade et al. (2020) conducted studies in reservoirs situated in the same region of Viçosa - MG and found similar results, with a vertical uncertainty of 0.4 m and 0.8 m respectively.

Moreover, numerous studies employ the NDWI for Satellite Derived Bathymetry, especially using for water body delineation in preprocessing (Misra & Ramakrishnan, 2020; Evagorou et al., 2022; Zhou et al., 2023). It is important to highlight that these studies found values close to those of the particular study for R^2 and RMSE, ranging from 70 to 90% and 0.70 to 2.00 m, respectively.

Furthermore, it should be emphasized that numerous factors can influence the construction of the index and consequently the prediction of depth, such as the radiometric resolution of the sensor. Therefore, this technique should be employed with caution and does not completely replace the periodic execution of bathymetric surveys using acoustic systems.

3.2 Bathymetry extraction method by ANNs

From the radiance values inserted in the Artificial Neural Network for the training, it was possible to obtain the following network configurations for A150, A250, A500, and Atraditional, respectively.

The network contains six input layers (from blue, green, red, and near-infrared bands and X and Y coordinates) and three hidden layers. In addition, it is important to remember that for the correct algorithm functioning, the data entered were normalized at first.

Subsequently, the authors conducted the modeling based on universal kriging, obtaining the Digital Depth Model similar to the method applied with the NDWI index. Finally, through the generated DDMs, the volume calculation was performed for each spacing in question and the Atraditional (Atrad). Table 5 summarizes the values obtained compared to the volume found with the Reference Bathymetry.

Table 5: Calculated model volumes for A150, A250, A500, Atraditional (Atrad), and reference bathymetry.

	Volume (m^3)	Difference with the reference method (m^3)	Difference with the reference method (%)
A150	110,302.03	4,601.74	4%
A250	93,824.78	21,078.99	18%
A500	86,568.32	28,335.45	25%
Atrad	113,380.32	1,523.45	1%
Reference Bathymetry	114,903.770	-	-

Considering the volumes found, shown in Table 5, it can be seen that the volume obtained with the sections spaced 500 to 500 meters (A500) was the one that showed the greatest discrepancy from the others, as occurred for NDWI.

For the spaced sections of 150 meters, the obtained volume differed by only 4% from the reference, and for Atrad (using random points), the volume found was even better, with a difference of only 1% from the actual reservoir volume.

Studies such as the one presented by Andrade et al. (2022) show that neural networks tend to yield better predictions when a greater number of points are used for training, as is the case with Atrad and A150.

In the same way that it was used in applying the NDWI index for a complete analysis of the depth' vertical quality, the MAIB algorithm was used in a sample of random points. This way, it was possible to obtain an exploratory analysis for the discrepancies after excluding outliers according to the algorithm (Table 6).

Table 6: Exploratory analysis of discrepancies for the method with ANNs.

	A150	**A250**	**A500**	**Atrad**
Nº of observations	2107	1590	946	5522
Mean (m)	0.682	0.669	0.809	0.359
Minimum (m)	0.000	0.000	0.000	0.000
Maximum (m)	3.734	3.098	3.879	2.421
Variance (m^2)	0.281	0.190	0.381	0.119
Kurtosis coefficient	1.369	1.271	1.344	2.344
Asymmetry coefficient	1.125	0.820	1.155	1.681

According to Table 6, the data follow a symmetrical distribution according to the asymmetry and platykurtic coefficients since the kurtosis coefficients are less than 3.

The next step consisted of verifying the data independence through the experimental semivariogram. In the methodology proposed by Ferreira (2018), four semivariograms are first constructed, with ranges adjusted according to the best scale for the maximum distance. Thus, by analyzing these graphs, it was possible to conclude that the discrepancies are spatially dependent.

The execution of the Block Bootstrap technique can be performed after verifying the data dependency. This tool was applied following the number of replications cited in the method with the NDWI, establishing 5,000 new data sets, with the block diagonal adjusted to values equivalent to the range of the experimental semivariogram for each spacing (150, 250, 500, and the method traditional). The graphs and histograms generated by the algorithm are found in Supplementary Materials E, F, G, H.

Sample biases were calculated from the discrepancy between the estimated uncertainty through the original sample and the median of the Bootstrap data. Table 7 illustrates these biases, the vertical uncertainty for each estimator, and the confidence interval.

Table 7: Vertical uncertainty for the method with ANN at the 95% confidence level and Bootstrap bias.

	Estimator	Vertical uncertainty (m)	$IC_{95\%}$	Sample bias
A150	RMSE	0.748	(0.744 - 0.752)	0.052
	Φ	0.748	(0.744 - 0.752)	0.052
	Φ_{Robust}	0.722	(0.719 - 0.732)	0.057
A250	RMSE	0.785	(0.782-0.790)	0.013
	Φ	0.785	(0.782-0.790)	0.013
	Φ_{Robust}	0.803	(0.796-0.808)	0.011
A500	RMSE	1.148	(1.144 – 1.158)	-0.132
	Φ	1.148	(1.144 – 1.158)	-0.132
	Φ_{Robust}	1.158	(1.144 – 1.166)	-0.074
Atrad	RMSE	0.489	(0.480 - 0.497)	0.011
	Φ	0.489	(0.480 - 0.497)	0.011
	Φ_{Robust}	0.335	(0.327 - 0.343)	0.030

Note that for the method using sections of 250 in 250 meters (A250), the smallest bias was found for the samples, with a Φ of 80 cm. The Atrad method presents a lower vertical uncertainty, reaching values of 49 cm with a bias of 0.011. A150 also performs well with an uncertainty of 75 cm and a Φ_{Robust} of 72 cm.

Finally, it is noteworthy that according to the algorithm, the points used in the sections of 500 to 500 meters (A500) showed a lower convergence in the network training, with an error considerably greater than the other methods. This may be due to the low number of points used to train the neural network, which may have led to a low learning rate (POPESCU et al., 2009).

Authors such as Chu et al. (2023) employed Artificial Neural Networks (ANN) in three distinct areas in China and observed Root Mean Square Error (RMSE) values close to 40 cm for depths up to 4 m and approximately 1 m for deeper regions. They further emphasize the importance of proper selection of learning rate and weights to mitigate the issue of local minimum.

Similarly, Zhou et al. (2023) compared the backpropagation algorithm (ANN) with the Stumpf Method, Random Forest (RF), and Support Vector Machine. They found an average RMSE of 1.46 m for ANN and 1.41 m for RF. However, for deeper locations, the backpropagation algorithm of ANN exhibited lower vertical uncertainty when compared to RF and other algorithms. Nevertheless, there are no studies addressing the utilization of bathymetric sections for algorithm training, which would minimize the upfront effort of data acquisition. Being one of the main contributions of this research to the scientific community.

From this perspective, it is presumable that, in this study, the method used in A150 is efficient for extracting bathymetry with satellite images of the uncertainty in this method. Also, the volume was close to that obtained with the traditional method of randomly spaced points and the volume obtained with the reference bathymetry.

3.3 The final comparison between the methods and the respective sections

To make a broad comparison of the methods mentioned, three random bathymetric sections were constructed to compare, through profiles, the estimated depth with the different methods and the reference depth acquired with an echo sounder (Figure 5).

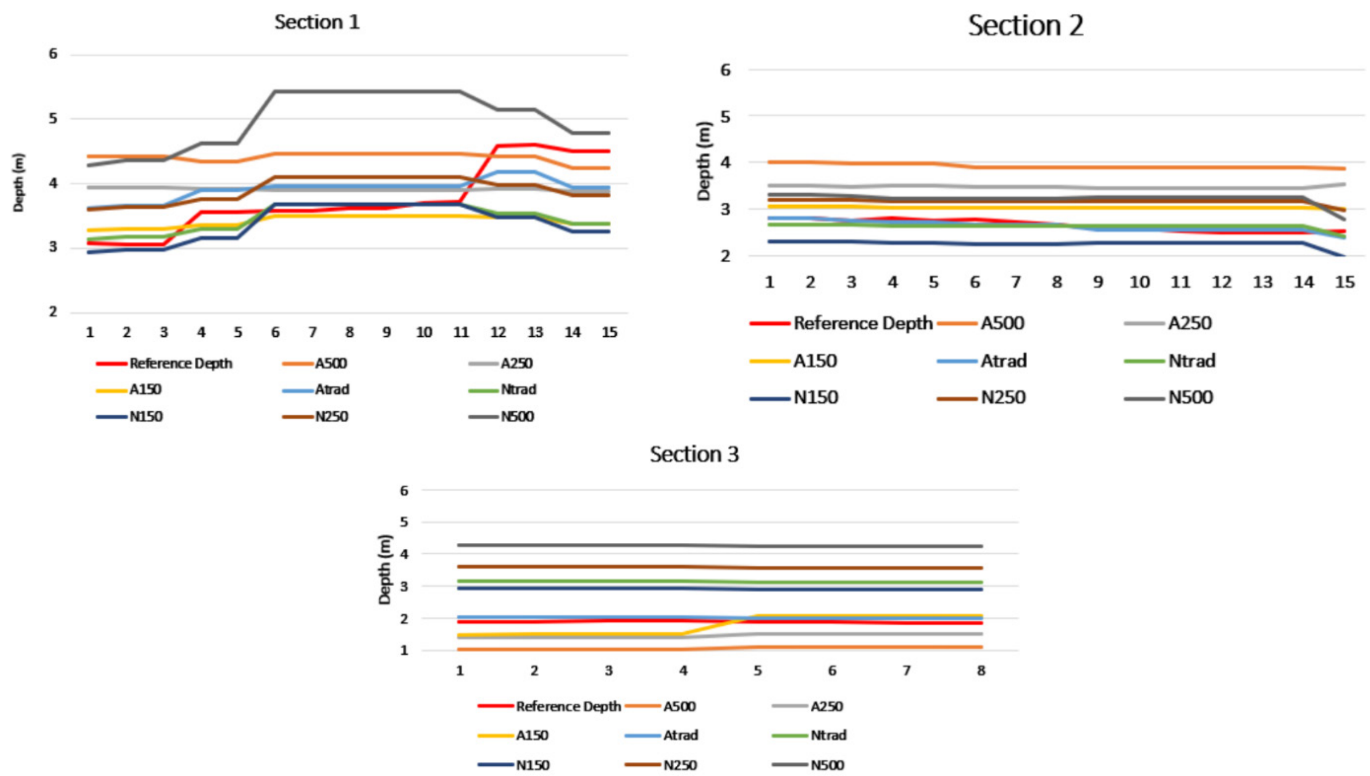

Figure 5: Comparison profiles between the resulting models.

As seen in Figure 5, the methods shown present small displacements in the depth value concerning the reference depth, especially in section 2, where there was little depth change. It is important to highlight that Ntrad and N150 presented similar behavior in all sections, and Atrad exhibited the closest adherence to the Reference Depth.

In section 1, where the depth varies from 3.0 m to almost 5.0m, the A250 and N250 methods were the ones that showed the smallest overall discrepancies from the reference depth, followed by Atrad, A150, N150, and Ntrad. In this section, the method that exhibited the worst performance was N500, reaching depth values greater than 5.0 meters.

In Section 2, both Atrad and Ntrad closely followed the reference depth profile, while A150 exhibited a similar trend to the reference depth, with overestimated values in the range of 10 to 40 cm. Conversely, N150 exhibited the opposite, as the depths were underestimated.

In Section 3, where the depth remains nearly constant, the Artificial Neural Network (ANN) outperformed all the methods studied. The most discrepant value was observed for A500, with a difference of approximately 1.00 m, while for A150 and Atrad, this difference was less than 30 cm.

From this information, as well as the values obtained for the vertical uncertainties and volumes for each method, the superiority of the neural network over NDWI is evident, especially about randomly spaced points in the study area (Atrad).

4. Conclusion

The bathymetry extraction was evaluated using a high-resolution image through sections of bathymetric points trained. The result showed a better estimate of the sections spaced from 150 meters using ANN methods, with a difference in the volume of only 4% for the reference bathymetry.

It is well known that the traditional method for satellite-derived bathymetry estimation, using empirical approaches, remains relatively costly due to the high quantity of in-situ data points that must be acquired. In this regard, the methodology proposed in this study, utilizing Artificial Neural Networks (ANNs), demonstrates the feasibility of employing spaced 150-meter sections in water bodies with relatively low uncertainties consistent with volume estimation. This substantially reduces the number of pre-collected data points.

It can be asserted that this methodology is valid, particularly for preliminary environmental studies, as well as for assessing sedimentation or erosion in a water body, provided that the study area does not have a high concentration of suspended sediments or aquatic vegetation. These factors can hinder light penetration and consequently alter the radiance values of the pixels.

It is worth noting that for narrower water bodies when employing the NDWI index, it is advisable to use a dataset with a higher spatial resolution to represent the bottom without interference from other spectral natures.

For future research, it is recommended to apply this methodology to different water bodies using other Machine Learning algorithms, employing the spaced sections for training. This approach streamlines the initial bathymetric survey, making it less time-consuming and cost-effective.

ACKNOWLEDGMENT

This work was carried out with the support of GPHidro – Grupo de Pesquisa em Levantamentos Hidrográficos at the Federal University of Viçosa and CNPq - Conselho Nacional de Desenvolvimento Científico e Tecnológico.

AUTHOR’S CONTRIBUTION

Laura Coelho de Andrade: Conceptualization, methodology, data analysis, drafting; Letícia Perpétuo Pinheiro: Conceptualization, methodology, data analysis, drafting; Italo Oliveira Ferreira: Data analysis, writing - revision, final approval; Nilcilene das Graças Medeiros: Literature review, data analysis, editing; Arthur Amaral e Silva: Review, editing.

REFERENCES

ANDRADE, L. C.; FERREIRA, Í. O.; MEDEIROS, N. D. G.; FONSECA, I. G. R. D. *Viabilidade do uso de imagens de RPA’s para extração da batimetria em reservatórios de água rasos*. 2020.

ANDRADE, L. C.; FERREIRA, I. O.; MEDEIROS, N.G.; TEIXEIRA, V. G.; SANTOS, F. C. M. Evaluation of Images Obtained with the Micasense Sensor in the Estimation of Bathymetry in Shallow Optically Water Bodies. *Brazilian Journal of Cartography*, [S. l.], v. 73, n. 2, p. 615–633, 2021. DOI: 10.14393/rbcv73n2-55439.

ANDRADE, L.C.; FERREIRA, Í.O.; SANTOS, F.C.M.; OLIVEIRA, J.C. Evaluation of probabilistic interpolators for better water management of water bodies. Proceedings of the VII Brazilian Symposium on Geodetic Sciences and Geoinformation Technologies, Recife, pp.172-181. 2018.

ANDRADE, L.C; FERREIRA, Í.O.; AMARAL E SILVA, A.; GIBRIM, V. T.; SANTOS, F.C.M. On the use of artificial neural networks in remotely piloted aircraft acquired images for estimating reservoir’s bathymetry. *Bulletin of Geodetic Sciences*. 28(1): e2022006, 2022. DOI: 10.1590/s1982-21702022000100006

ANA - Agência Nacional de Águas. *Orientações para atualização das curvas cota x área x volume*. Superintendência de Gestão da Rede Hidrometeorológica. Brasília: ANA, SGH.2013.

CAMBARDELLA, C. A.; MOORMAN, T. B.; NOVAK, J. M.; PARKIN, T. B.; KARLEN, D. L.; TURCO, R. F.; KONOPKA, A. E. Field scale variability of soil properties in Central Iowa soils. *Soil Science Society of America Journal*, Madison, v. 58, n. 5, p. 1501-1511, 1994.

CANDELA, C, R. Estimativa da profundidade de corpos de água com o uso de dados de sensoriamento remoto. Dissertação (Mestrado). Programa de Pós-Graduação em Engenharia Civil, Universidade Federal de Santa Catarina, Florianópolis, Santa Catarina, 141p., 2013.

CHU, S.; CHENG, L.; CHENG, J.; ZHANG, X.; ZHANG, J.; CHEN, J.; LIU, J. Shallow water bathymetry based on a back propagation neural network and ensemble learning using multispectral satellite imagery. *Acta Oceanologica Sinica,* 42(5), 154-165. 2023.

DHAWAN, V. Water and agriculture in India. In Background paper for the South Asia expert panel during the Global Forum for Food and Agriculture (Vol. 28, pp. 80-85). OAV German Asia-Pacific Business Association.2017.

EL-MEWAFI, M.; SALAH, M.; FAWZI, B. Assessment of optical satellite images for bathymetry estimation in shallow areas using artificial neural network model. Am. J. Geogr. Inf. Syst, 7, 99-106.2018.

EVAGOROU, E.; ARGYRIOU, A.; PAPADOPOULOS, N.; METTAS, C.; ALEXANDRAKIS, G.; HADJIMITSIS, D. Evaluation of satellite-derived bathymetry from high and medium-resolution sensors using empirical methods. Remote Sensing, 14(3), 772.2022.

FERREIRA, I. O. Quality control in hydrographic surveys. Thesis (Doctorate). Graduate Program in Civil Engineering, Department of Civil Engineering, Federal University of Viçosa, Viçosa, Minas Gerais, 216p., 2018.

FERREIRA, Í. O., OLIVEIRA, J. C. D., SANTOS, A. D. P. D., SILVA, A. A., & MEDEIROS, N. D. G. Point To Point: An Alternative Method For Extracting “Homologous Points” In Bathymetric Data Collected With A Multibeam System. Bulletin of Geodetic Sciences. 27.2021.

FERREIRA, I. O.; NETO, A. A.; MONTEIRO, C. S. The use of unmanned vessels in bathymetric surveys. Revista Brasileira de Cartografia, v. 68, n. 10, 2016a.

FERREIRA, I. O.; RODRIGUES, D. D.; SANTOS, G. R. Study on the Appropriate Use of Kriging in the Computational Representation of Bathymetric Surfaces. Revista Brasileira de Cartografia (Online), Rio de Janeiro, no 65/5, p.831-842, 2013.

FERREIRA, Í. O.; RODRIGUES, D. D.; SANTOS, G. R.; Collection, processing and analysis of bathymetric data. 1st ed. Saarbrucken: New Academic Editions, v. 1, 100p., 2015.

FERREIRA, Í. O.; ZANETTI, J.; GRIPP, J. S.; MEDEIROS, N.G. Feasibility of using Rapideye system images to determine shallow water bathymetry. Brazilian Journal of Cartography, 68(7).2016b.

FOERSTNOW, L. P.; MENEZES, J. T. Applicability of satellite images using NDWI to determine the bathymetry of Lagoa da Conceição, Florianópolis, SC. Brazilian Symposium on Remote Sensing XV-SBSR, Curitiba.2011.

GIORDANO, F.; MATTEI, G.; PARENTE, C.; PELUSO, F.; SANTAMARIA, R. Integrating Sensors Into. A Marine Drone for Bathymetric 3d Surveys in Shallow Waters. Sensors, V. 16, N. 1, P. 41, 2015.

GUO, X.; JIN, X.; JIN, S. Shallow water bathymetry mapping from ICESat-2 and Sentinel-2 based on BP neural network model. Water, 14(23), 3862.2022.

HALLSWORTH, J. E. Water is a preservative of microbes. Microbial Biotechnology, 15(1), 191-214.2022

HAMDY, A. Water use efficiency in irrigated agriculture: an analytical review. Water use efficiency and water productivity: WASAMED project, 9-19. 2007.

HUANG, Yiqun; Lars J. Kangas & Barbara A. Rasco. Applications of Artificial Neural Networks (ANNs) in Food Science. Critical Reviews in Food Science and Nutrition, 47:2, 113-126.2007. DOI: 10.1080/10408390600626453

HYPACK, Inc. Hypack – Hydrographic Survey Software User Manual. Middletown, USA, 1784p., 2018.

IHO-International Hydrographic Organization. Manual on Hydrography. Mônaco: International Hydrographic Bureau. 540p. 2005.

JACKSON, R. B., Carpenter, S. R., Dahm, C. N., McKnight, D. M., Naiman, R. J., Postel, S. L., & Running, S. W. Water in a changing world. Ecological applications, 11(4), 1027-1045.2001.

JONG, C.D.; LACHAPELLE, G.; SKONE, S.; ELEMA, I.A. Hydrography. 2ª Ed. Delft University Press: Vssd. 354p. 2010.

KALOOP, M. R.; EL-DIASTY, M.; HU, J. W.; ZARZOURA, F. Hybrid artificial neural networks for modeling shallow-water bathymetry via satellite imagery. IEEE Transactions on Geoscience and Remote Sensing, 60, 1-11.2021.

KRUG, L. A.; NOERNBERG, M. A. Remote Sensing as a Tool for Determining Shoal Bathymetry in Baía das Laranjeiras, Paranaguá-PR. Brazilian Journal of Geophysics, v. 25, pp. 101-105, 2007. DOI: 10.1590/S0102-261X2007000500010.

LEGLEITER, C.J.; ROBERTS, D.A.; LAWRENCE, R.L. Spectrally based remote sensing of river bathymetry. Earth Surf. Process. Landforms 2009, 34, 1039–1059. Available online: https://onlinelibrary.wiley.com/doi/pdf/10.1002/esp.1787

LIMA, J. R. C; SHINOZAKI, R; ALMEIDA, A. Q; RODRIGUES, C. T. A. Estimation of the bathymetry of the Saco dam - PE with remote sensing data. Anais IV Regional Symposium on Geoprocessing and Remote Sensing - Geonordeste, Aracaju. 2012.

MA Y, XU N, LIU Z, YANG B, YANG F, WANG XH, LI S. Satellite-derived bathymetry using the ICESat-2 lidar and Sentinel-2 imagery datasets. Remote Sensing of Environment. Dec 1; 250:112047.2020.

MANLEY, J. E. Unmanned surface vehicles, 15 years of development. In: OCEANS 2008, IEEE, p.1-4,2008.

MARTINI, L. Topografia Aplicada aos Levantamentos Hidrográficos. Department of Geomatics. Earth Sciences Sector, Federal University of Paraná. Curitiba, Paraná.2007.

MATOS A. J. S. Qualitative improvements in the modeling of bathymetric surveys in reservoirs using the computational tool “CAV-NH”. Postgraduate thesis in Environmental Engineering Sciences at the School of Engineering of São Carlos - University of São Paulo. São Carlos, 2012.

MCFEETERS, S. K. The use of the Normalized Difference Water Index (NDWI) in the delineation of open water features. International Journal of Remote Sensing, v. 17, n. 7, p. 1425-1432, 1996.

MISRA, A.; RAMAKRISHNAN, B. Assessment of coastal geomorphological changes using multi-temporal Satellite-Derived Bathymetry. Continental Shelf Research, 207, 104213.2020.

PIAO, S., CIAIS, P., HUANG, Y., SHEN, Z., PENG, S., LI, J. & FANG, J. The impacts of climate change on water resources and agriculture in China. Nature, 467(7311), 43-51. 2010.

PLANET, Planet Imagery Product Specification: PlanetScope & Rapideye, 2016.URL: https://www.planet.com/products/satellite-imagery/files/1610.06_Spec%20Sheet_Combined_

POPESCU, M. C.; BALAS, V. E.; PERESCU-POPESCU, L.; MASTORAKIS, N. Multilayer perceptron and neural networks. WSEAS Transactions on Circuits and Systems, v. 8, n. 7, p. 579-588, 2009.

QADDUMI, H. Practical approaches to transboundary water benefit sharing. Vol. 292. London: Overseas Development Institute, 2008.

R CORE TEAM. R: A language and environment for statistical computing. R Foundation for Statistical Computing, Vienna, Austria. 2020.

RIBEIRO, S.R.A.; CENTENO, J.A.S.; KRUEGER, C. P. Depth estimation from bathymetric survey and IKONOS II data using artificial neural networks. Bulletin of Geodetic Sciences, v. 14, n. 2, p. 171-185, 2008.

SANTOS, D, FERNÁNDEZ-FERNÁNDEZ S, ABREU T, SILVA PA, BAPTISTA P. Retrieval of nearshore bathymetry from Sentinel-1 SAR data in high energetic wave coasts: The Portuguese case study. Remote Sensing Applications: Society and Environment.25:100674.2022.

SANTOS, F. C. M.; FERREIRA, I. O.; ANASTACIO, L. C.; OLIVEIRA, J. C. Use of optical remote sensing to estimate the silting up of water reservoirs. In: Brazilian Symposium on Geodetic Sciences and Geoinformation Technologies, 2018, Recife. Anais do VII SIMGEO. Recife: Editora UFPE. v. 1. p. 936-944. 2018.

SILVA, J. F. A.; PEREIRA, R. G. Global overview of freshwater distribution and use. Ibero-American Journal of Environmental Sciences, v. 10, n. 3, p. 263-280, 2019. URL: http://doi.org/10.6008/CBPC2179-6858.2019.003.0023

VIEIRA, S. R. Geostatistics in soil spatial variability studies. In. NOVAES, R. F.; ALVAREZ V., V. H.; SCHAEFER, C. E G. R. Topics in soil science. Viçosa, MG: Brazilian Society of Soil Science, v.1. p.2-54, 2000.

WARRICK, A.W. & NIELSEN, D.R. Spatial variability of soil physical properties in the field. In: HILLEL, D. Applications of soil physics. New York: Academic Press, p.319-344, 1980.

YANG, X. et al. Mapping of urban surface water bodies from sentinel-2 msi imagery at 10 m resolution via NDWI - based image sharpening. Remote Sensing. 2017.

ZANI, H.; ASSINE, M. L.; SILVA, A. Fluvial bathymetry estimated with orbital data: case study in the upper course of the Paraguay River with the aster sensor. Geosciences (São Paulo), v. 27, n. 4, p. 555-565, 2008.

ZHOU,W.; TANG, Y.; JING, W.;LI, Y.; YANG, J.; DENG, Y.; ZHANG, Y. A Comparison of Machine Learning and Empirical Approaches for Deriving Bathymetry from Multispectral Imagery. Remote Sens. 2023, 15, 393. https://doi.org/10.3390/rs15020393